

Supplementary Information

Topochemically Constructed Heterogeneous Flexible Vanadium-based
Electrocatalyst for Boosted Conversion Kinetics of Polysulfides in Li-S Batteries

Yadong Yang¹, Xingxing Li¹, Rongjie Luo¹, Xuming Zhang¹, Jijiang Fu¹, Yang Zheng^{1*}, Kaifu Huo^{3*},
Tengfei Zhou^{2,4*}

¹ The State Key Laboratory of Refractories and Metallurgy, Institute of Advanced Materials and
Nanotechnology, Wuhan University of Science and Technology, Wuhan 430081, China

² Institutes of Physical Science and Information Technology, Anhui University, Hefei, 230601, China

³ Wuhan National Laboratory for Optoelectronics (WNLO), School of Optical and Electronic
Information, Huazhong University of Science and Technology, Wuhan 430074, China

⁴ Institute for Superconducting and Electronic Materials (ISEM), Australian Institute for Innovative
Materials (AIIM), School of Mechanical, Materials, Mechatronics and Biomedical Engineering,
University of Wollongong, Wollongong, 2522, Australia

*Corresponding authors:

E-mail: yzheng@wust.edu.cn (Y. Zheng); kfhuo@hust.edu.cn (K.F. Huo); tengfeiz@uow.edu.au (T.F. Zhou);

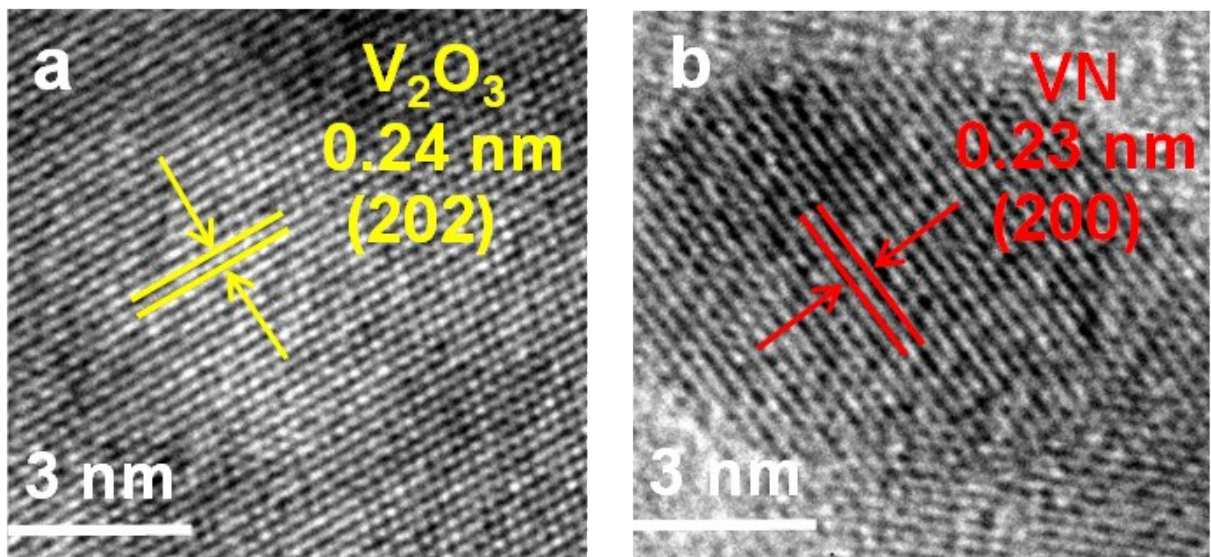


Figure S1. (a) HRTEM image of the V₂O₃@VN-0. (b) HRTEM image of the V₂O₃@VN-60.

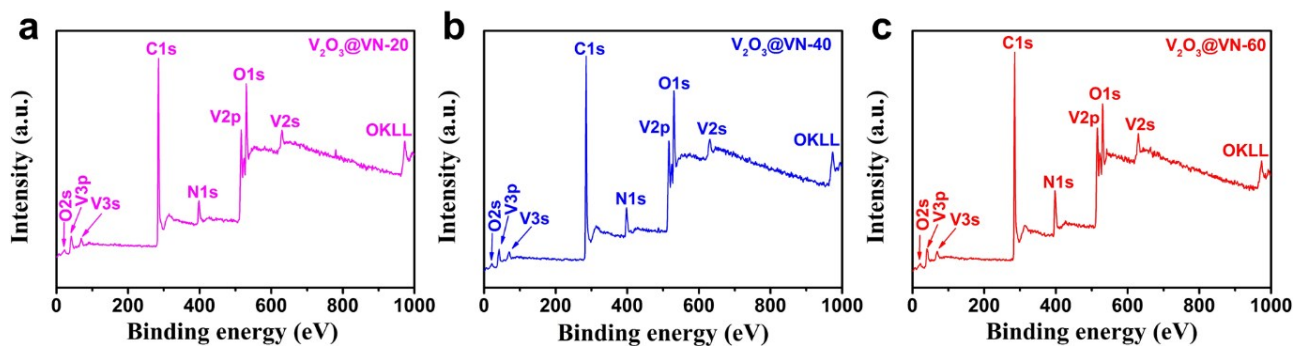


Figure S2. XPS full-scan spectrum of the (a)V₂O₃@VN-20, (b) V₂O₃@VN-40, and (c) V₂O₃@VN-60.

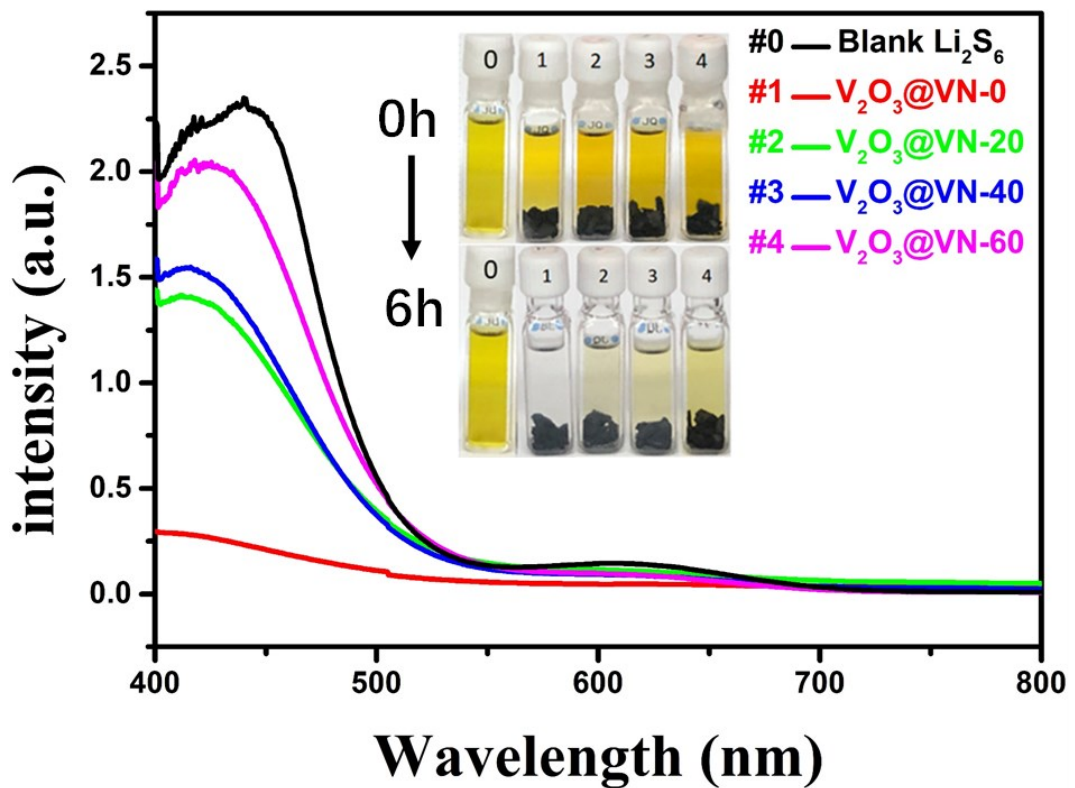


Figure S3. Li_2S_6 adsorption test. 0: bare Li_2S_6 solution. 1: $\text{V}_2\text{O}_3@\text{VN}-0$. 2: $\text{V}_2\text{O}_3@\text{VN}-20$. 3: $\text{V}_2\text{O}_3@\text{VN}-40$. 4: $\text{V}_2\text{O}_3@\text{VN}-60$.

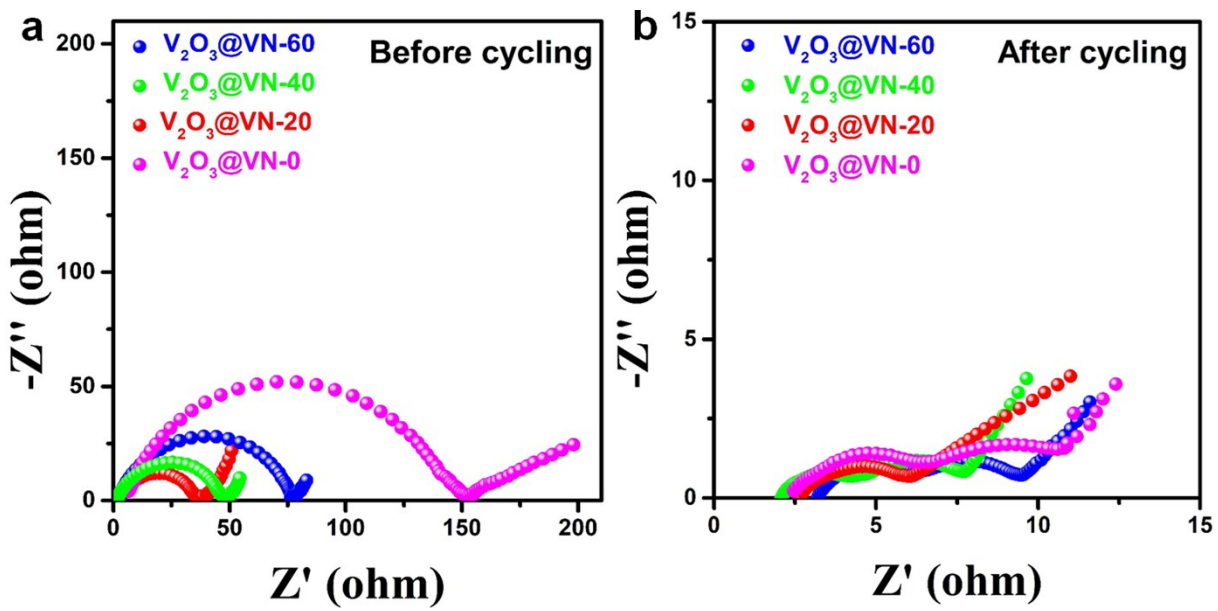


Figure S4. (a) Nyquist plots for the batteries before cycles. (b) Nyquist plots for the batteries after cycles.

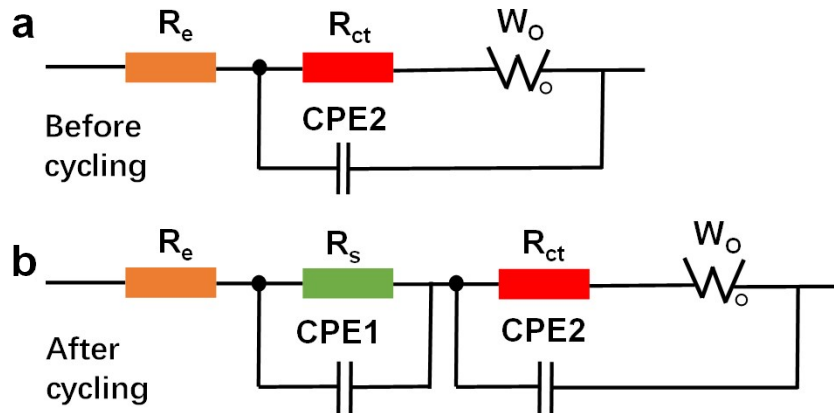


Figure S5. The EIS equivalent circuit of $\text{V}_2\text{O}_3@\text{VN-0}$, $\text{V}_2\text{O}_3@\text{VN-20}$, $\text{V}_2\text{O}_3@\text{VN-40}$, and $\text{V}_2\text{O}_3@\text{VN-60}$ electrodes for Li-S batteries, while (a) the fresh cell without the process of R_s and its relevant CPE1, (b) can be applied to the battery after cycling. R_e : The internal resistance of the electrolyte; R_s : The internal resistance of the solid electrolyte interface (SEI) film correlated with the insoluble $\text{Li}_2\text{S}_2/\text{Li}_2\text{S}$; R_{ct} : The charge-transfer resistance, related to the electrode reaction kinetics; CPE1: Capacitance of the electrode bulk in high-frequency region; CPE2: Capacitance of the charge transfer process at the interface between the sulfur and electrolyte; W_o : The semi-infinite Warburg diffusion impedance of the long-chain LiPSSs.

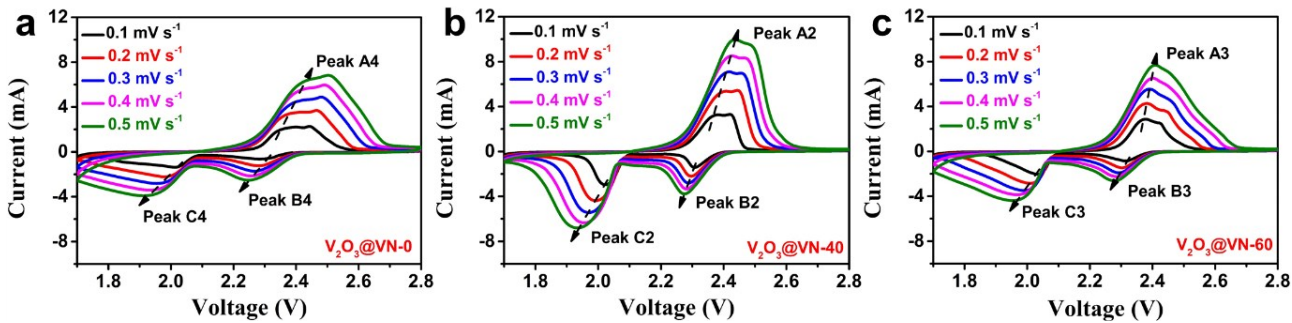


Figure S6. CV curves of the (a) V_2O_3 @VN-0, (b) V_2O_3 @VN-40, and (c) V_2O_3 @VN-60 electrodes under various scan rates of 0.1-0.5 mV s⁻¹ within the voltage window from 1.7 to 2.8 V.

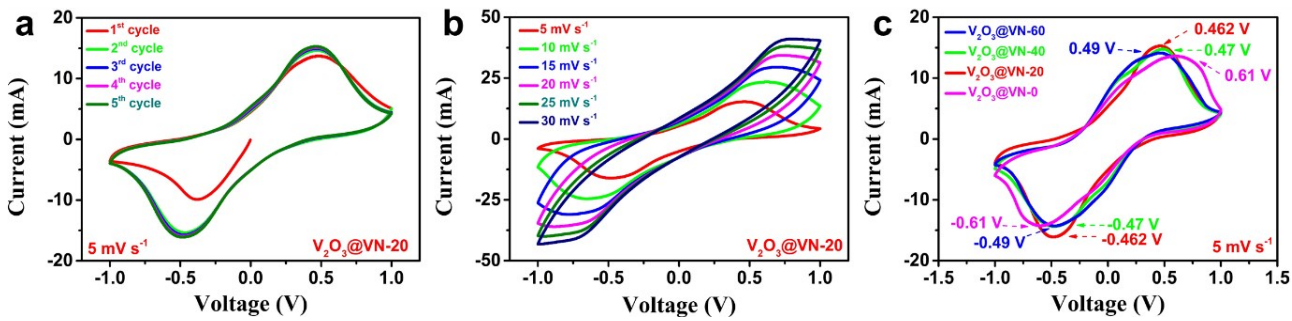


Figure S7. (a) Multi-cycles CV curves of V_2O_3 @VN-20 symmetric battery at 5 mV s⁻¹. (b) CV curves of the V_2O_3 @VN-20 symmetric cell at different scan rates of 5-30 mV s⁻¹. (c) Comparison CV curves of V_2O_3 @VN-0, V_2O_3 @VN-20, V_2O_3 @VN-40 and V_2O_3 @VN-60 symmetric battery at 5 mV s⁻¹.

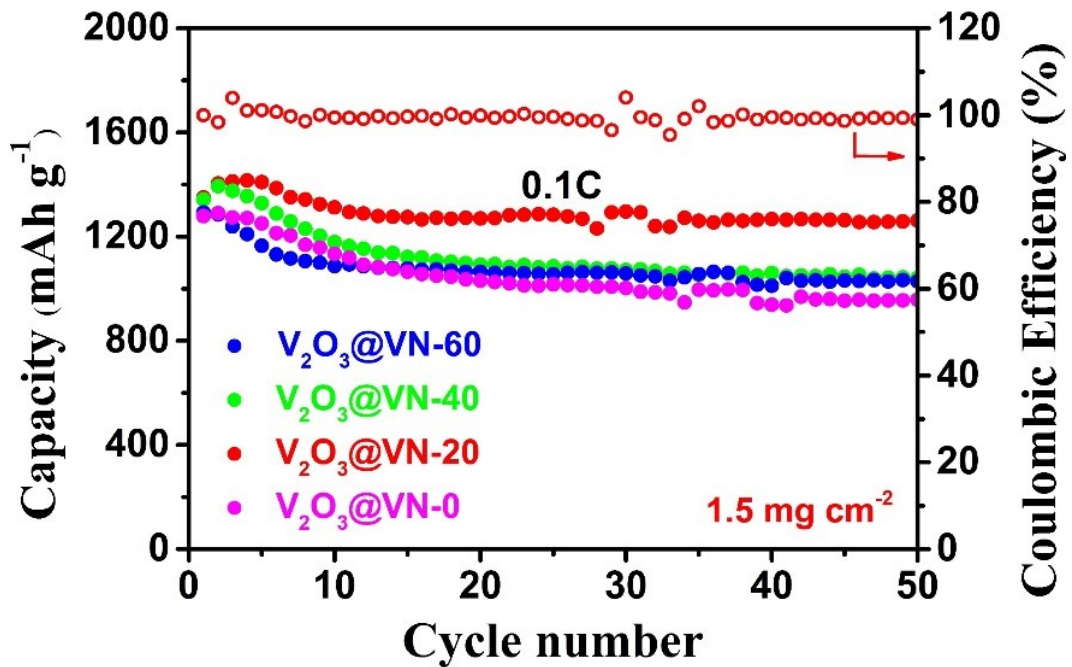


Figure S8. Cycling performances of the V_2O_3 @VN-0, V_2O_3 @VN-20, V_2O_3 @VN-40, and V_2O_3 @VN-60 cathodes at 0.1 C.

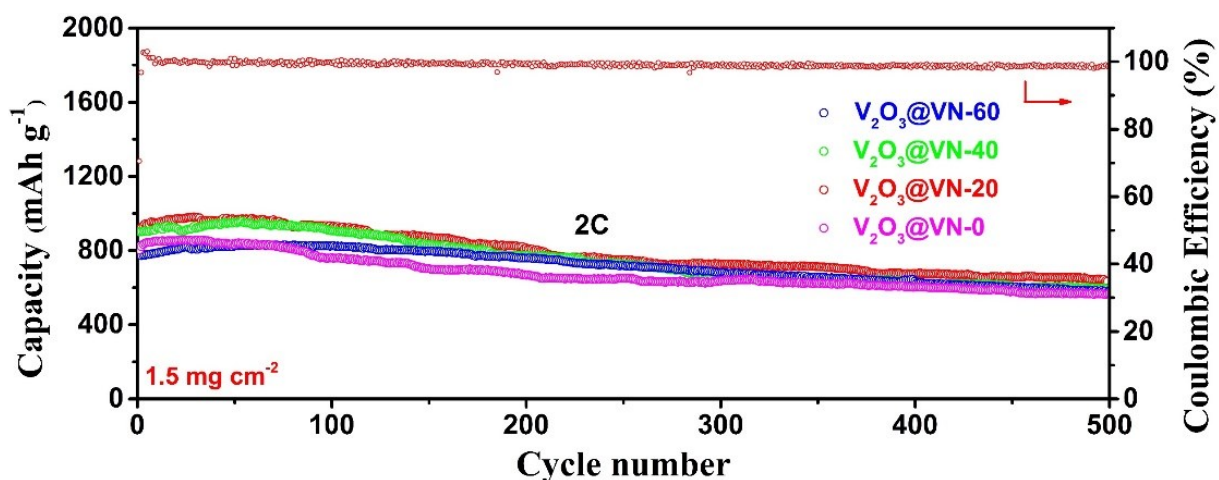


Figure S9. Long-term cycling performances of the V_2O_3 @VN-0, V_2O_3 @VN-20, V_2O_3 @VN-40, and V_2O_3 @VN-60 cathodes at 2 C.

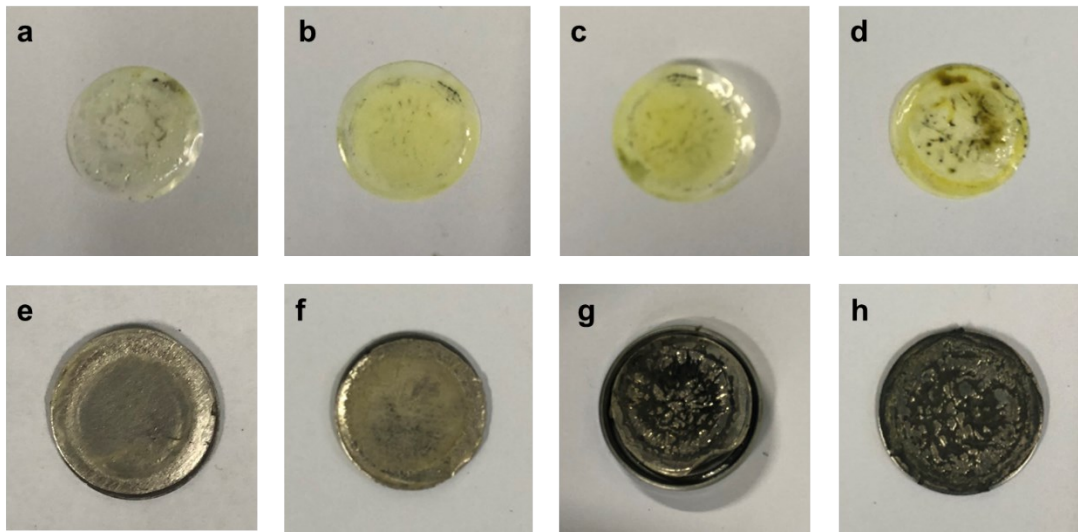


Figure S10. Photographs of the separators of the cycled cells with (a) $\text{V}_2\text{O}_3@\text{VN-20}$, (b) $\text{V}_2\text{O}_3@\text{VN-40}$, (c) $\text{V}_2\text{O}_3@\text{VN-60}$, and (d) $\text{V}_2\text{O}_3@\text{VN-0}$. Photographs of the cycled lithium foil (after 300 cycles at 5C) from cells paired with (e) $\text{V}_2\text{O}_3@\text{VN-20}$, (f) $\text{V}_2\text{O}_3@\text{VN-40}$, (g) $\text{V}_2\text{O}_3@\text{VN-60}$ and (h) $\text{V}_2\text{O}_3@\text{VN-0}$.

Table S1. Impedance parameters of the EIS spectra of the V₂O₃@VN-0, V₂O₃@VN-20, V₂O₃@VN-40, and V₂O₃@VN-60 electrodes before cycling.

Sample	R _e (Ω)	R _{ct} (Ω)	Sum(Ω)
V ₂ O ₃ @VN-0	6.44	153	159.44
V ₂ O ₃ @VN-20	2.59	34.21	36.8
V ₂ O ₃ @VN-40	1.93	46.67	48.6
V ₂ O ₃ @VN-60	2.66	75.04	77.7

Table S2. Impedance parameters of the EIS spectra of V₂O₃@VN-0, V₂O₃@VN-20, V₂O₃@VN-40 and V₂O₃@VN-60 electrodes after cycling.

Sample	R _e (Ω)	R _s (Ω)	R _{ct} (Ω)	Sum(Ω)
V ₂ O ₃ @VN-0	2.45	3.97	4.18	10.60
V ₂ O ₃ @VN-20	2.78	1.53	1.68	5.99
V ₂ O ₃ @VN-40	2.22	2.20	1.91	6.33
V ₂ O ₃ @VN-60	3.35	2.65	2.64	8.64

Table S3. Comparation of battery performances based on sulfur hosts between this work and other reported studies.

Host materials	Mass loading of S (mg cm ⁻²)	Initial capacity (mAh g ⁻¹) 1) /Current density (C)	Capacity retention rate (%) / Cycles	Rate Capability (mAh g ⁻¹) /Current density (C) at mass loading of S (mg cm ⁻²) 2)	Ref.
V ₂ O ₃ @VN-20	3	860 / 1C	78.3 % / 200	793 / 5 at 1.5	This work
V ₂ O ₃ @VN-20	5	888 / 0.5C	95.1 % / 100		This work
3VO ₂ -1VN	2.8	800 / 1C	64 % / 100	800 / 5 at 1.6	1
VN/C	2.8	1200 / 1C	61 % / 200	650 / 5 at 2.8	2
7TiN: 3TiO ₂ -G	3.1	503 / 1C	73 % / 2000	682 / 2 at 1	3
GA-VOx	1.8	600 / 1C	96.4 % / 200	442 / 2 at 1.8	4
TiO ₂ /rGO	1	800 / 1C	43.1 % / 200	606 / 2 at 1.5	5
VN@C	4.2	900 / 1C	65.8 % / 300	581 / 5 at 1.2	6
TiN-S-G	3.4	500 / 1C	80.4 % / 500	644 / 2 at 1.1	7
Co ₄ N	1.5	1640 / 1C	60.9 % / 100	600 / 5 at 1.5	8
VN/CA	1.3	1038 / 1C	77.2% / 100	901 / 2 at 1.3	9
VN-NB	3.3	988 / 0.5	96% / 200	837 / 2 at 3.3	10
CNTs/Co ₃ S ₄ -NBs	1.2	954 / 1	99.2% / 500	702 / 5 at 1.2	11
CNTs/CoS-NSs	1	982 / 1	72 % / 500	573 / 5 at 1	12
Co@NCNP/NCNT	4	857 / 0.09	70 % / 500	479 / 0.3 at 4	13
NGCM	1.3	829 / 1	79 % / 500	593 / 3 at 1.3	14

References

- Y. Song, W. Zhao, L. Kong, L. Zhang, X. Zhu, Y. Shao, F. Ding, Q. Zhang, J. Sun, Z. J. E. Liu and E. Science, *Energy & Environmental Science*, 2018, **11**, 2620-2630.
- X. Li, K. Ding, B. Gao, Q. Li, Y. Li, J. Fu, X. Zhang, P. K. Chu and K. J. N. E. Huo, *Nano Energy*, 2017, **40**, 655-662.
- T. Zhou, W. Lv, J. Li, G. Zhou, Y. Zhao, S. Fan, B. Liu, B. Li, F. Kang, Q.-H. J. E. Yang and E. Science, *Energy & Environmental Science*, 2017, **10**, 1694-1703.
- Y. Zhang, X. Ge, Q. Kang, Z. Kong, Y. Wang and L. J. C. E. J. Zhan, *Chemical Engineering Journal*, 2020, 124570.
- J. Song, J. Zheng, S. Feng, C. Zhu, S. Fu, W. Zhao, D. Du and Y. J. C. Lin, *Carbon*, 2018, **128**, 63-69.
- L. Zhu, C. Li, W. Ren, M. Qin and L. J. N. J. o. C. Xu, *New Journal of Chemistry*, 2018, **42**, 5109-5116.
- B. Hao, H. Li, W. Lv, Y. Zhang, S. Niu, Q. Qi, S. Xiao, J. Li, F. Kang and Q.-H. J. N. E. Yang, *Nano Energy*, 2019, **60**, 305-311.
- D.-R. Deng, F. Xue, Y.-J. Jia, J.-C. Ye, C.-D. Bai, M.-S. Zheng and Q.-F. J. A. n. Dong, *ACS nano*, 2017, **11**, 6031-6039.
- X. Li, R. Tang, K. Hu, L. Zhang and Z. J. E. A. Ding, *Electrochimica Acta*, 2016, **210**, 734-742.
- L. Ma, H. Yuan, W. Zhang, G. Zhu, Y. Wang, Y. Hu, P. Zhao, R. Chen, T. Chen and J. Liu, Porous-shell vanadium

- nitride nanobubbles with ultrahigh areal sulfur loading for high-capacity and long-life lithium–sulfur batteries, *Nano letters*, 2017, **17**, 7839-7846.
- 11. T. Chen, Z. Zhang, B. Cheng, R. Chen, Y. Hu, L. Ma, G. Zhu, J. Liu and Z. Jin, Self-templated formation of interlaced carbon nanotubes threaded hollow Co₃S₄ nanoboxes for high-rate and heat-resistant lithium–sulfur batteries, *Journal of the American Chemical Society*, 2017, **139**, 12710-12715.
 - 12. L. Ma, W. Zhang, L. Wang, Y. Hu, G. Zhu, Y. Wang, R. Chen, T. Chen, Z. Tie and J. Liu, Strong capillarity, chemisorption, and electrocatalytic capability of crisscrossed nanostraws enabled flexible, high-rate, and long-cycling lithium–sulfur batteries, *ACS nano*, 2018, **12**, 4868-4876.
 - 13. W. Yan, J. Wei, T. Chen, L. Duan, L. Wang, X. Xue, R. Chen, W. Kong, H. Lin and C. Li, Superstretchable, thermostable and ultrahigh-loading lithium–sulfur batteries based on nanostructural gel cathodes and gel electrolytes, *Nano Energy*, 2021, **80**, 105510.
 - 14. L. Ma, G. Zhu, W. Zhang, P. Zhao, Y. Hu, Y. Wang, L. Wang, R. Chen, T. Chen and Z. Tie, Three-dimensional spongy framework as superlyophilic, strongly absorbing, and electrocatalytic polysulfide reservoir layer for high-rate and long-cycling lithium-sulfur batteries, *Nano Research*, 2018, **11**, 6436-6446.